



Cell-to-Cell Transmission Is the Main Mechanism Supporting Bovine Viral Diarrhea Virus Spread in Cell Culture

Fernando Merwaiss,^a Cecilia Czibener,^a Diego E. Alvarez^a

^aInstituto de Investigaciones Biotecnológicas, Conicet, Universidad Nacional de San Martín, Argentina

ABSTRACT After initiation of an infective cycle, spread of virus infection can occur in two fundamentally different ways: (i) viral particles can be released into the external environment and diffuse through the extracellular space until they interact with a new host cell, and (ii) virions can remain associated with infected cells, promoting the direct passage between infected and uninfected cells that is referred to as direct cell-to-cell transmission. Although evidence of cell-associated transmission has accumulated for many different viruses, the ability of members of the genus *Pestivirus* to use this mode of transmission has not been reported. In the present study, we used a novel recombinant virus expressing the envelope glycoprotein E2 fused to mCherry fluorescent protein to monitor the spreading of bovine viral diarrhea virus (BVDV) (the type member of the pestiviruses) infection. To demonstrate direct cell-to-cell transmission of BVDV, we developed a cell coculture system that allowed us to prove direct transmission from infected to uninfected cells in the presence of neutralizing antibodies. This mode of transmission requires cell-cell contacts and clathrin-mediated receptor-dependent endocytosis. Notably, it overcomes antibody blocking of the BVDV receptor CD46, indicating that cell-to-cell transmission of the virus involves the engagement of coreceptors on the target cell.

IMPORTANCE BVDV causes one of the most economically important viral infections for the cattle industry. The virus is able to cross the placenta and infect the fetus, leading to the birth of persistently infected animals, which are reservoirs for the spread of BVDV. The occurrence of persistent infection has hampered the efficacy of vaccination because it requires eliciting levels of protection close to sterilizing immunity to prevent fetal infections. While vaccination prevents disease, BVDV can be detected if animals with neutralizing antibodies are challenged with the virus. Virus cell-to-cell transmission allows the virus to overcome barriers to free virus dissemination, such as antibodies or epithelial barriers. Here we show that BVDV exploits cell-cell contacts to propagate infection in a process that is resistant to antibody neutralization. Our results provide new insights into the mechanisms underlying the pathogenesis of BVDV infection and can aid in the design of effective control strategies.

KEYWORDS CD46, E2, bovine viral diarrhea virus, cell-to-cell transmission, endocytosis, pestiviruses, reporter genes, surface receptor, virus entry

Bovine viral diarrhea virus (BVDV) is a positive-strand RNA virus that infects cattle and causes major economic losses to the livestock industry worldwide (1). Together with classical swine fever virus (CSFV) and border disease virus (BDV) of sheep, BVDV belongs to the *Pestivirus* genus in the family *Flaviviridae*. The family also comprises flaviviruses, which are arthropod-borne viruses, including important human pathogens such as dengue virus, yellow fever virus, and tick-borne encephalitis virus; hepaciviruses, including hepatitis C virus (HCV); and pegiviruses (2). Virus genomes contain a single open reading frame (ORF) that is translated into a polyprotein. For pestiviruses,

Citation Merwaiss F, Czibener C, Alvarez DE. 2019. Cell-to-cell transmission is the main mechanism supporting bovine viral diarrhea virus spread in cell culture. *J Virol* 93:e01776-18. <https://doi.org/10.1128/JVI.01776-18>.

Editor Susana López, Instituto de Biotecnología/UNAM

Copyright © 2019 American Society for Microbiology. All Rights Reserved.

Address correspondence to Diego E. Alvarez, dalvarez@iibintech.com.ar.

Received 6 October 2018

Accepted 24 October 2018

Accepted manuscript posted online 7 November 2018

Published 17 January 2019

the polyprotein is cleaved by viral and cellular proteases into the following individual viral proteins: N^{pro}-C-E^{ns}-E1-E2-p7-NS2-NS3-NS4A-NS4B-NS5A-NS5B (3, 4). Pestivirus particles consist of a lipid bilayer with envelope glycoproteins E^{ns}, E1, and E2 surrounding the nucleocapsid, composed of the capsid protein C and the RNA genome (5, 6). E2 determines the cellular tropism of the virus, which is directly related to the interaction of E2 and cellular receptors (7, 8). In turn, it has been shown that a soluble version of the E2 protein inhibits viral infection and that E2 is the main antigenic determinant of infection and induces the production of neutralizing antibodies (9–11).

Cytopathic (cp) and noncytopathic (ncp) biotypes of BVDV differ in their capacity to induce cell death in culture (12). Adult cattle are most commonly infected by ncpBVDV biotypes that cause acute infections and can cross the placenta of the dam to infect the fetus, leading to congenital malformations and abortion or to the birth of persistently infected (PI) animals. PI animals are immunotolerant to BVDV and shed the virus, spreading the disease in cattle populations (13, 14). cpBVDV biotypes arise in PI cattle, from recombination events in the infecting ncpBVDV genome, and are associated with the development of fatal mucosal disease (15, 16). BVDV control requires combining vaccination with removal of PI animals. While vaccination is effective at the herd level, it is not completely effective in every individual animal (10). In fact, animals with neutralizing antibodies can develop viremia and shed virus in nasal secretions when challenged with the homologous virus (17, 18). However, the strategies that BVDV uses to overcome the host antibody response still remain unclear.

The viral infection cycle begins with the entry of free viral particles into susceptible cells through interaction with receptors and coreceptors that trigger clathrin-mediated endocytosis, allowing the internalization of the virion in an endosomal vesicle (19–21). A pH drop in the endosome triggers the fusion of virus and the cell membranes, which results in the release of genomic RNA into the cytoplasm of the infected cell (22–24). It has been shown for many enveloped viruses that, after initiation of an infective cycle, spread of infection can occur by two different mechanisms. On the one hand, progeny viruses are released from the cell and diffuse through the extracellular space until they interact with a new host cell. Alternatively, virions can remain associated with infected cells and propagate to neighboring cells at sites of direct cell-cell contact (25–27). The latter mode of spreading is known as direct cell-to-cell transmission. There are many attractive advantages associated with direct cell-to-cell transmission that can be exploited by viruses. In general, cell-associated transmission is considered more rapid and efficient because it obviates rate-limiting steps of cell-free spread: the cycle of release, diffusion, and entry can occur quickly at cell-cell contact sites. Moreover, viruses that move across tight and adherens junctions are protected from the effects of neutralizing antibodies and other immune system components (28). Therefore, a common feature of cell-associated transmission of viruses is the ability to spread infection even in the presence of neutralizing antibodies, which completely block the entry of free viruses. In recent years, evidence has accumulated that many animal viruses can efficiently propagate through direct cell-to-cell transmission (29, 30). Neurotropic viruses exploit neurochemical synapses to spread between connected neurons. For instance, herpesvirus membrane proteins engage kinesin motors for anterograde transport of vesicles containing fully assembled virus particles toward axon termini. Virus egress involves fusion of the transport vesicle with the axonal membrane at the exit sites (31). Other viruses induce the formation of cell-cell contacts, referred to as virological synapses, through the interaction of virus glycoproteins with receptors on the target cell. Next, the assembly and egress of the viral progeny become polarized toward contact sites. For HIV, integrins and intercellular adhesion molecules surround virological synapses, and polarization of virus assembly is directed by the rearrangement of the cytoskeleton and the secretory machinery (32). Viruses that use actin polymerization as a driving force for spread include murine leukemia virus and vaccinia virus (30). The murine leukemia virus envelope glycoprotein engages receptors on the target cell to establish filopodial bridges that transport the virus toward the noninfected cell (33). On the other hand, the extracellular form of vaccinia virus that remains associated with the infected

cell induces polymerization of actin tails that propel the virus toward the target cell (34). Within the *Flaviviridae* family, it has been reported that cell-to-cell transmission of HCV depends on the expression of two host proteins that also function as postattachment receptors for the entry of free virus, namely, claudin-1 and occludin, both of which are present in tight junction cell-cell contacts (35–38).

So far, the ability of any member of the genus *Pestivirus* to spread directly from infected to noninfected cells has not been reported. In the present study, we developed a novel recombinant BVDV strain expressing the envelope glycoprotein E2 fused to mCherry fluorescent protein that allowed us to monitor the spread of infection. Using a fluorescence microscopy-based approach to quantify spreading of the reporter virus in a coculture of producer and target cells expressing fluorescent proteins of contrasting colors, we demonstrated the ability of BVDV to propagate in the presence of antibodies that neutralize free viruses. Furthermore, our approach unambiguously shows that direct transmission from cell to cell requires the interaction of E2 with cell receptors and clathrin-mediated endocytosis by the target cell.

RESULTS

Development of a reporter virus expressing a fusion of mCherry to E2 envelope protein. Different recombinant pestiviruses have been developed that express foreign genes as reporter proteins that are released from the viral polyprotein by proteolytic cleavage and serve to monitor viral infection (39–41). To follow the spread of BVDV infection in the present study, we designed a recombinant virus that carries a fusion of mCherry fluorescent protein to the E2 envelope protein. We constructed a pair of cytopathic and noncytopathic infectious clones in which the mCherry coding sequence is inserted between the protease cleavage site at the C terminus of E1 and the beginning of E2 (Fig. 1A). Tagging of E2 at this position was previously shown to have no impact on BVDV growth kinetics and particle formation (42, 43). Next, full-length genomic RNAs were synthesized by *in vitro* transcription, using the recombinant infectious clones as templates, and transfected into MDBK cells. Three days after RNA transfection, mCherry expression was detected by fluorescence microscopy for both cp- and ncpBVDV/mCherry-E2 (Fig. 1B and data not shown). Immunostaining with an NS3 antibody was used to detect BVDV replication and showed that the NS3 antibody-stained cells expressed mCherry, indicating that recombinant RNAs were competent for viral replication. Next, we collected supernatants of transfected cells and infected a new monolayer of MDBK cells to assess the production of infectious viruses (Fig. 1C). The day after infection, expression of mCherry was readily observed under a fluorescence microscope and was confined to single cells for both cytopathic and noncytopathic viruses. At 2 days, the cytopathic virus formed large foci of infection, and cytopathic effect was evident 3 days after infection. In turn, spread of infection by the noncytopathic virus resulted in an intact monolayer of cells expressing mCherry by day 3. In addition, we used confocal microscopy to evaluate the degree of colocalization between mCherry and E2 in cells infected with the recombinant virus and stained with a monoclonal antibody (MAb) against E2. Image analysis produced Pearson and Manders coefficients that indicated colocalization between mCherry and antibody staining signals, suggesting that mCherry remains fused to E2 (Fig. 1D). Finally, to address the impact of mCherry insertion on the production of infectious virus, we compared the specific infectivities of RNAs transcribed from parental or BVDV/mCherry-E2 infectious clones (44). The viral titers determined at 2 days for the supernatants of MDBK cells transfected with equal amounts of the RNAs were similar, suggesting that fusion of mCherry to E2 does not significantly impact the assembly of infectious particles. Altogether, these results confirm that the N terminus of E2 is a suitable site for the insertion of foreign proteins into the pestivirus genome.

BVDV/mCherry-E2 uses the authentic entry pathway of BVDV for entry into MDBK cells. Interaction of the BVDV envelope protein E2 with cell-specific receptors triggers clathrin-mediated endocytosis, and acidification of the endosomal compartment is required for release of the genome into the cytoplasm of the infected cell

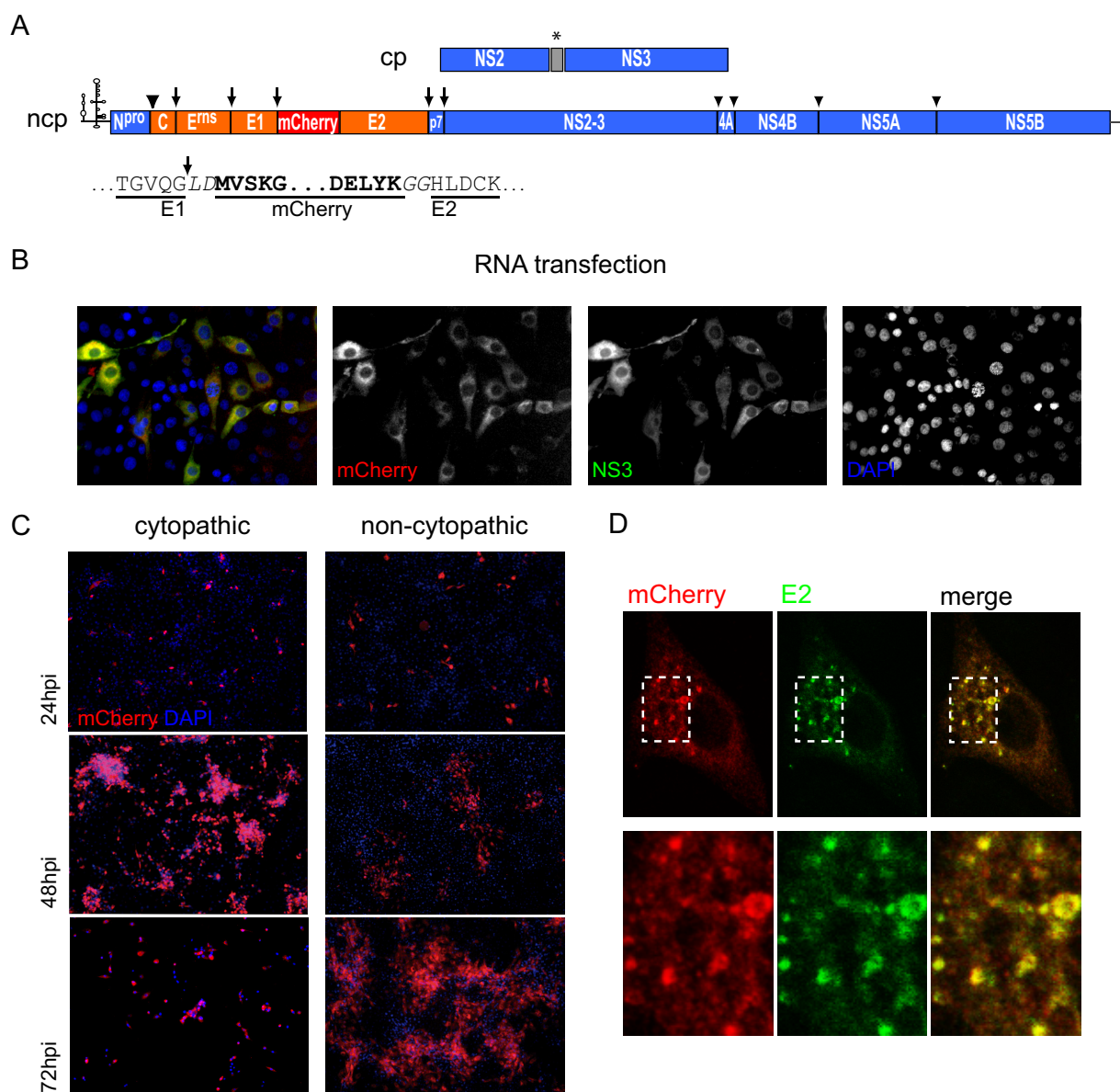


FIG 1 Design and construction of recombinant BVDV carrying a fusion of mCherry fluorescent protein to the viral envelope protein E2. (A) Schematic representation of BVDV/mCherry-E2 genome. The mCherry sequence was inserted between the protease cleavage site at the end of E1 and the beginning of E2. Coding sequences for nonstructural proteins are indicated in blue and those for structural proteins in orange. Host signal peptidase cleavage sites are indicated with arrows and viral protease cleavage sites with arrowheads. (Top) Insertion of the 90-amino-acid DNAJC14 subdomain (Jiv90) within NS2 into the cytopathic (cp) variant of BVDV/mCherry-E2 is indicated with a gray box. (Bottom) Sequence of amino acids around the mCherry insertion. (B) mCherry expression coincides with NS3 expression. Representative images of MDBK cells transfected with *in vitro*-transcribed RNA of BVDV/mCherry-E2 are shown. Cells were fixed at 3 days posttransfection and stained with a monoclonal antibody against NS3 and with DAPI. (C) Time course of infection of MDBK cells with cytopathic and noncytopathic BVDV/mCherry-E2. Images of fixed cells stained with DAPI were acquired at 24, 48, and 72 h postinfection. (D) mCherry colocalizes with E2. Confocal microscopy images of MDBK cells infected with BVDV/mCherry-E2 and stained with a monoclonal antibody against E2 are shown. Split-channel images of the boxed areas are presented in the bottom row. Colocalization analysis values are as follows: Pearson's *R*, 0.68; Manders M1, 0.959; Manders M2, 0.984; and Costes *P*, 1.00.

(19–21). Given that insertion of mCherry at the N terminus of E2 might affect the function of the envelope protein, altering the entry route of the recombinant virus, we compared the sensitivities of parental BVDV and BVDV/mCherry-E2 to different chemical and molecular entry inhibitors. In order to evaluate the use of BVDV receptors, we employed a soluble version of E2, obtained using a baculovirus system for recombinant expression, to compete with the entry of the virus (Fig. 2A and B). The recombinant protein reduced BVDV cytopathic effect in a dose-dependent manner, reaching total

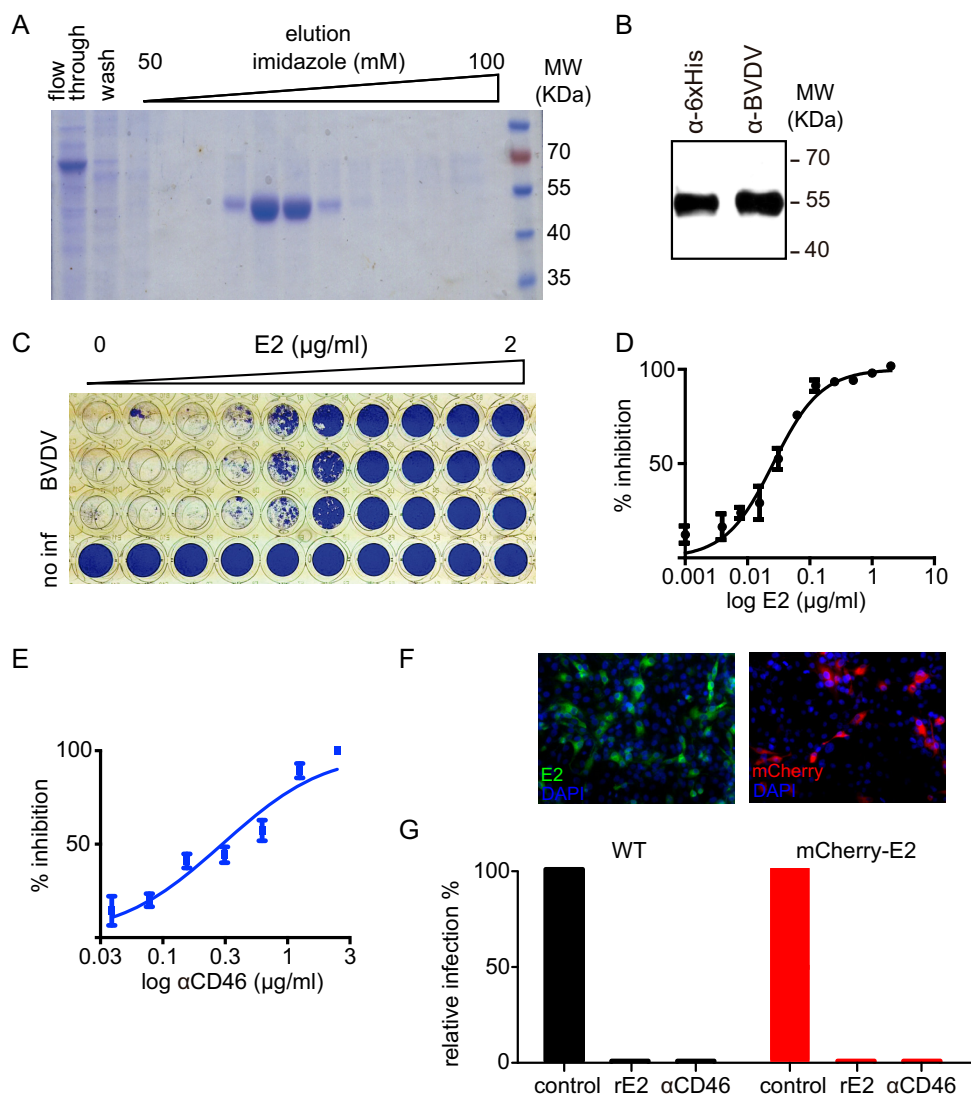


FIG 2 Soluble E2 and MAbs against CD46 block BVDV infection. (A) Expression of recombinant E2. A truncated version of E2 fused to a 6×His tag at the C terminus was produced in a soluble form by use of a baculovirus expression system and purified by affinity chromatography. Fractions eluted from an IMAC column with increasing concentrations of imidazole were resolved by SDS-PAGE, and elution of the recombinant protein was detected by Coomassie blue staining of the gel. (B) Western blotting using anti-6×His tag (left lane) and anti-BVDV (right lane) antibodies confirmed the identity of the protein. (C) Functionality of recombinant E2 tested in a cytopathic effect reduction assay. MDBK cells were preincubated with increasing amounts of the recombinant protein and then infected with cpBVDV at an MOI of 0.01 (BVDV; top rows) or left uninfected (no inf; bottom row). At 3 to 4 days postinfection, cells were fixed and stained with crystal violet to estimate the extent of the cytopathic effect. (D) Inhibition of BVDV infection by recombinant E2. Data collected from the cytopathic effect reduction assay were used to plot the log concentration versus the percentage of inhibition. Inhibitory concentrations were estimated from nonlinear regression fitting of the curve. (E) Plot of the log concentration versus the percentage of inhibition for cytopathic effect reduction assay of BVDV infection in MDBK cells preincubated with increasing amounts of a mix of MAbs BVD/CA 17 and 26 against CD46. (F) Representative images of cells infected with parental BVDV or BVDV/mCherry-E2 and fixed at 24 h. Cells infected with the parental virus were identified by immunostaining of E2 (green channel in left panel). Expression of mCherry allowed direct visualization of cells infected with BVDV/mCherry-E2 (red channel in right panel). (G) Soluble E2 and CD46 MAbs completely inhibited infection by parental BVDV and BVDV/mCherry-E2. The bar graph shows the quantification of the inhibition of BVDV entry into MDBK cells preincubated with recombinant E2 (rE2) or CD46 MAbs (αCD46). Cells were infected with parental BVDV or BVDV/mCherry-E2 and processed as described for panel F. Bars represent the percentages of infected cells relative to control cells for infection with parental BVDV (WT; black bars) or BVDV/mCherry-E2 (red bars).

inhibition at 1 μg/ml (Fig. 2C and D). In addition, to address the usage of a BVDV-specific cell receptor, we used MAbs against CD46 to block virus infection (8) (Fig. 2E). The inhibitory effects of recombinant E2 or CD46 MAbs on parental BVDV and BVDV/mCherry-E2 infection were compared in MDBK cells that were incubated with either the

soluble protein or the antibodies before infection with the virus. At 24 h postinfection, entry was assessed by fluorescence microscopy using E2 antibody staining or mCherry expression to detect infection with parental or recombinant virus, respectively (Fig. 2F). We observed that both soluble E2 and CD46 MAbs completely blocked entry for parental BVDV and BVDV/mCherry-E2 (Fig. 2G). Next, we evaluated the dependence on clathrin-mediated endocytosis and acidification of the endosomal compartment for internalization by using chlorpromazine and ammonium chloride treatments, respectively. MDBK cells were pretreated with increasing amounts of chlorpromazine or ammonium chloride for 1 h before infection and then infected in the presence of the drug. After 2 h, cells were washed to remove the drug and noninternalized viruses, and the effect of drug treatment on virus entry was quantified by fluorescence microscopy (Fig. 3A and data not shown). We observed for both viruses that entry was blocked to similar extents, and in a dose-dependent manner, in cells treated with chlorpromazine (Fig. 3B). Similar results were obtained for ammonium chloride treatment (Fig. 3C). To further confirm the endocytic internalization of the virus, we quantified entry of BVDV into cells expressing a control or dominant negative version of Eps15, which is specific for clathrin-mediated endocytosis. To this end, we transduced MDBK cells with lentiviruses expressing fusions of green fluorescent protein (GFP) to DIIIΔ2 (control) and EH29 (dominant negative) Eps15 constructs. Uptake of transferrin conjugated to Texas Red was used as a control for clathrin-dependent endocytosis. As expected, we observed that the fluorescent dye was efficiently internalized into cells expressing DIIIΔ2 Eps15, while internalization into cells expressing EH29 Eps15 was diminished (Fig. 3D), indicating that loss of clathrin-mediated endocytosis function is achieved by expressing the dominant negative construct in MDBK cells. In agreement with the results for chlorpromazine treatment, entry of both parental BVDV and BVDV/mCherry-E2 was blocked in MDBK cells expressing dominant negative Eps15 (Fig. 3E and F). Altogether, these results indicate that BVDV/mCherry-E2 uses the authentic entry pathway of BVDV to infect MDBK cells.

BVDV spread is resistant to antibody neutralization. Virus spread can rely on two mechanisms: release of free virus particles and direct cell-to-cell transmission, which is often resistant to antibody neutralization. To experimentally address whether cell-to-cell transmission contributes to dissemination of BVDV, we assayed spread in the presence of BVDV neutralizing antibodies. To this end, we first generated a BVDV neutralizing serum by immunizing mice with soluble protein E2. The serum showed a 90% neutralization titer (NT_{90}) of 10^4 and completely blocked infection with BVDV when preincubated with the virus stock (Fig. 4A and B). Antibodies of the IgG isotype purified from the serum and commercial monoclonal antibodies to E2 were also neutralizing, with estimated NT_{90} s of 10^3 and 10^4 , respectively (Fig. 4B). Next, we set up conditions to assess spreading of BVDV in the presence of neutralizing antibodies. MDBK cells were infected with BVDV/mCherry-E2, and at 2 h postinfection, noninternalized virus was removed by exhaustive washing and fresh medium or medium containing anti-E2 serum, IgG antibodies, or monoclonal antibodies was added (Fig. 4C). Imaging of infected cells at 2 days postinfection showed that the virus was able to spread both in the control and in the presence of neutralizing antibodies. However, spread was noticeably confined in the presence of neutralizing antibodies, as quantified by a significant reduction in the total percentage of infected cells compared to that for the control (Fig. 4D and E). To verify that dissemination of free viruses was blocked throughout the experiment, the supernatants of control cells and cells incubated in the presence of antibodies were collected at the end of the experiment and used to infect a new monolayer of MDBK cells. Infected cells were observed only after infection with the supernatant from control cells, indicating that free virus released from infected cells was completely neutralized in the assay (Fig. 4E). Therefore, the differences in the foci formed in the presence of neutralizing antibodies and in the control can be explained by free viruses not contributing to the spread of infection.

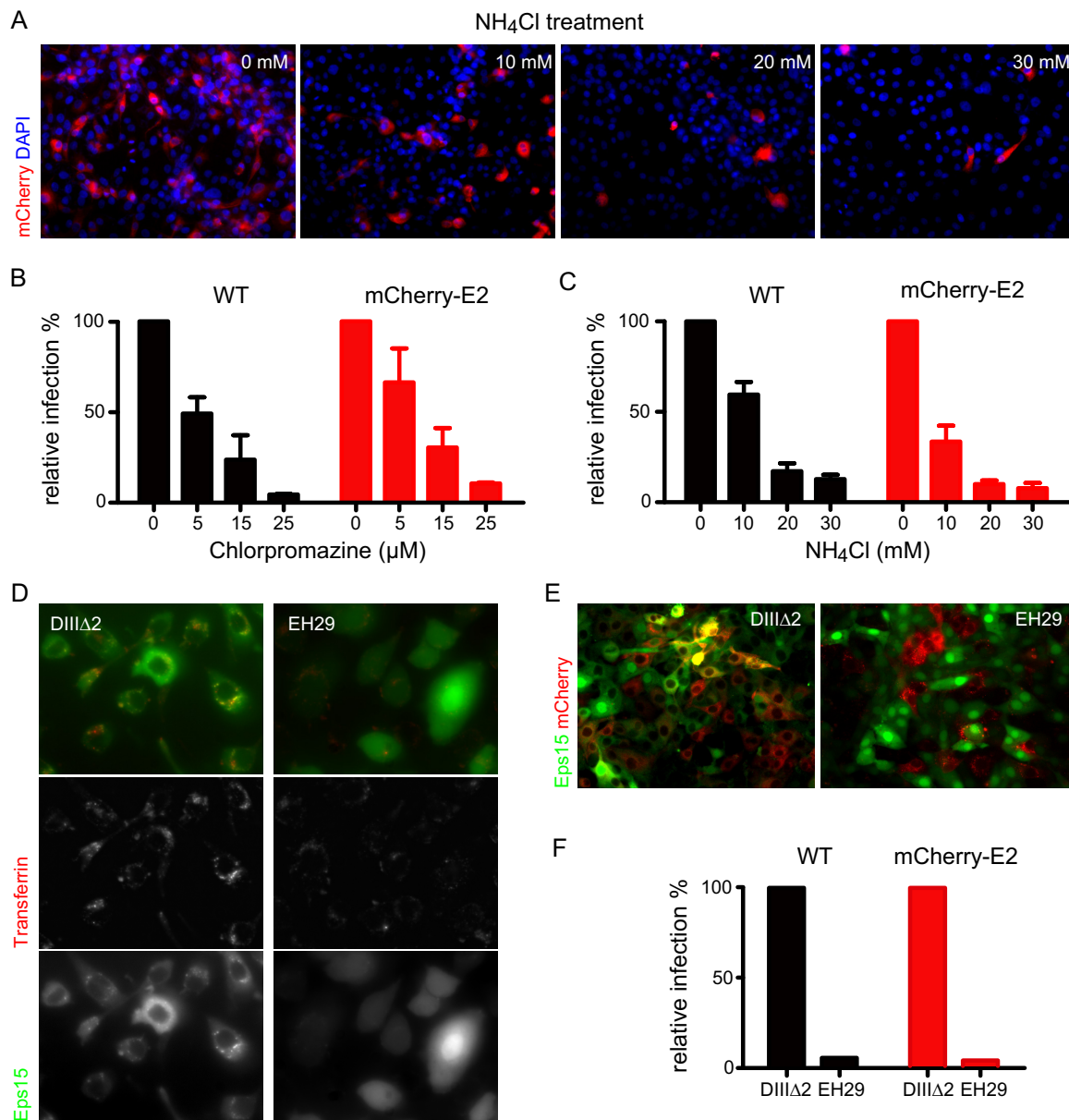


FIG 3 Comparison of the entry routes of parental BVDV and BVDV/mCherry-E2. (A) Effect of entry inhibitors on BVDV infection. Representative images of cells treated with increasing concentrations of NH₄Cl and infected with BVDV/mCherry E2 are shown. (B and C) Dose-dependent inhibition of BVDV entry by chlorpromazine and NH₄Cl. Bar graphs show the quantification of the inhibition of entry of parental BVDV or BVDV/mCherry-E2 into MDBK cells treated with increasing concentrations of drugs. Bars represent the means and standard deviations of the percentages of infected cells relative to control cells for three independent experiments. At least 500 infected cells were counted for the control in each of the experiments. (D) Overexpression of dominant negative Eps15 in MDBK cells decreases clathrin-dependent uptake of transferrin. Representative images of the uptake of Texas Red-labeled transferrin (red channel) into MDBK cells overexpressing a control (DIIIΔ2) or dominant negative (EH29) construct of Eps15 (green channel) are shown. (E) Representative images of the entry of BVDV/mCherry-E2 (red channel) into MDBK cells overexpressing a control (DIIIΔ2) or dominant negative (EH29) construct of Eps15 (green channel). (F) Overexpression of dominant negative Eps15 blocks infection with BVDV. The bar graph shows the quantification of virus entry into cells overexpressing a control (DIIIΔ2) or dominant negative (EH29) construct of Eps15. The percentage of cells overexpressing control Eps15 and infected with parental BVDV (black bars) or BVDV/mCherry-E2 (red bars) was set to 100%. Bars for cells overexpressing dominant negative Eps15 represent the percentage of infection relative to that for control Eps15-overexpressing cells.

To further confirm that spreading in the presence of neutralizing serum did not arise from cell-free dissemination of neutralization escape variants that might be present in the virus stock, we initiated infection by transfection of BVDV/mCherry-E2 RNA into MDBK cells. At 4 h posttransfection, cells were washed and infection was allowed to proceed for 2 days. In agreement with the results obtained after infection with virus

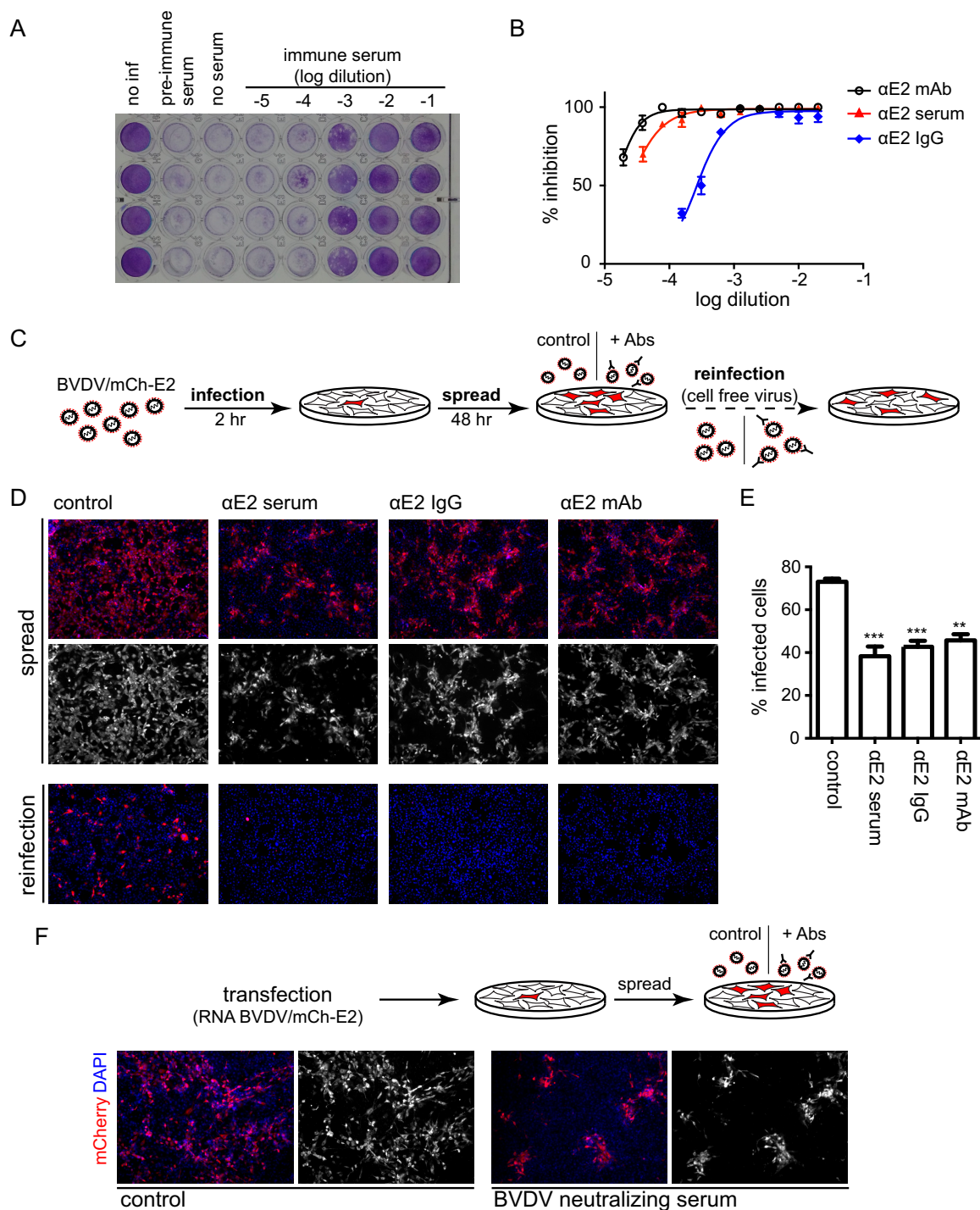


FIG 4 Spreading of BVDV is resistant to antibody neutralization of free viruses. (A) Titration of neutralizing antibodies by cytopathic effect reduction assay. An E2 immune serum was obtained from mice immunized with recombinant E2. A stock of cpBVDV was incubated with serial dilutions of the serum and then used to infect MDBK cells. At 3 to 4 days postinfection, cells were fixed and stained with crystal violet to estimate the extent of the cytopathic effect. (B) Data collected by cytopathic effect reduction assay were used to plot the log dilution versus the percentage of inhibition for serum against E2 (αE2 serum), the corresponding IgG fraction (αE2 IgG), and a MAb against E2 (αE2 MAb). Antibody titers were estimated from nonlinear regression fitting of the curve. (C) Schematic representation of the experimental setup to compare spreading of the virus in MDBK cells cultured in control medium or in the presence of neutralizing antibodies. (D) BVDV spread resists antibody neutralization of free virus. MDBK cells were infected with BVDV/mCherry-E2 (MOI = 0.1), and the infection was allowed to proceed for 48 h in control medium or in the presence of neutralizing antibodies. Representative images of virus spread (red channel) in cells cultured in control medium or medium containing neutralizing antibodies (top panels) and of the reinfection of fresh MDBK cells with the supernatants harvested at the end of the experiment (bottom panels) are shown. (E) Bar graph showing quantification of the absolute percentage of infected cells. Bars represent the means and standard deviations for three independent images. Data were analyzed by one-way ANOVA with Dunnett's posttest (**, $P < 0.01$; ***, $P < 0.001$). (F) (Top) Schematic representation of the experimental

(Continued on next page)

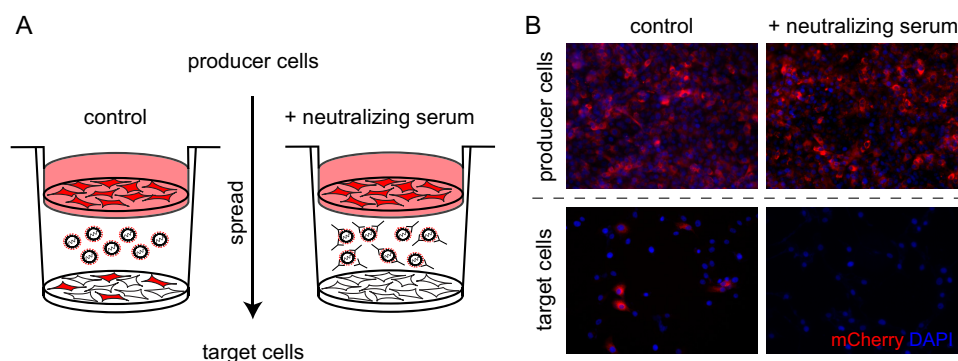


FIG 5 Antibody-resistant spreading of BVDV requires cell-cell contact. (A) Schematic representation of the transwell assay. Infected MDBK cells on a transwell membrane were cocultured with target MDBK cells in control medium or in the presence of neutralizing serum to test the dependence of spreading on cell-cell contact. (B) Representative images of the transwell assay for control spreading (left panels) and spreading in the presence of neutralizing serum (right panels). Producer cells were infected with BVDV/mCherry-E2 (red channel). Spreading from infected (producer) cells to noninfected (target) cells was assessed at 2 days postinfection.

stocks, spread of infection was observed both in the control and in the presence of neutralizing serum, and foci of infection were confined under the latter condition (Fig. 4F). Altogether, our results indicate that BVDV spread is resistant to antibody neutralization of free viruses.

Cell-to-cell transmission of viruses can occur across cell contact sites requiring direct contact of the primary infected cell with neighboring cells. To gain insight into the mechanism underlying spread of BVDV in the presence of neutralizing serum, we used a transwell coculture system to physically separate infected producer cells from target cells. Producer cells infected with BVDV/mCherry-E2 were plated on a cell culture insert, target cells were plated on the bottom of the well, and then the cells were cultured for 2 days in control medium or in medium containing neutralizing serum (Fig. 5A). Virus spread from producer to target cells was analyzed by fluorescence microscopy. As expected, infected target cells could be observed in the control transwell setup. In contrast, when neutralizing serum was added to the medium, no target cells were infected despite total infection of producer cells (Fig. 5B). Therefore, the results obtained by use of the transwell coculture system indicate that spread of BVDV in the presence of neutralizing antibodies requires direct cell-cell contact.

Direct cell-to-cell transmission is the main mechanism of BVDV spread. In order to unequivocally identify spread from infected producer cells to noninfected target cells, we set up a coculture system of producer MDBK cells persistently infected with the noncytopathic biotype of BVDV/mCherry-E2 and target MDBK cells stably expressing GFP, generated by lentivirus transduction and fluorescence-activated cell sorting. Producer and target cells were plated at a 1:4 ratio and cocultured in control medium or medium containing neutralizing antibodies (Fig. 6A). After 3 days, infection of target cells was evident in fluorescence microscopy images of cocultures. To quantify spreading, we devised an automated computer-assisted image analysis method (Fig. 6B and C) and used the ratio between the number of infected target cells and the total number of target cells as a measure of spreading from producer to target cells. Spreading was assessed using serum, purified IgG, or monoclonal antibodies to neutralize free virus. In all cases, we observed that spreading in the presence of neutralizing antibodies was reduced by around one-third with respect to the control level (Fig. 6D and E). On one hand, this result indicates that in the presence of antibodies the mechanism supporting spreading is the direct cell-to-cell transmission of the virus. On the other hand, since

FIG 4 Legend (Continued)

setup to assess virus spreading in the presence of neutralizing serum in an infection started by transfection of *in vitro*-transcribed RNA into MDBK cells. (Bottom) Representative images of cells transfected with the RNA of BVDV/mCherry-E2 (red channel) and cultured in control medium or in medium containing neutralizing serum.

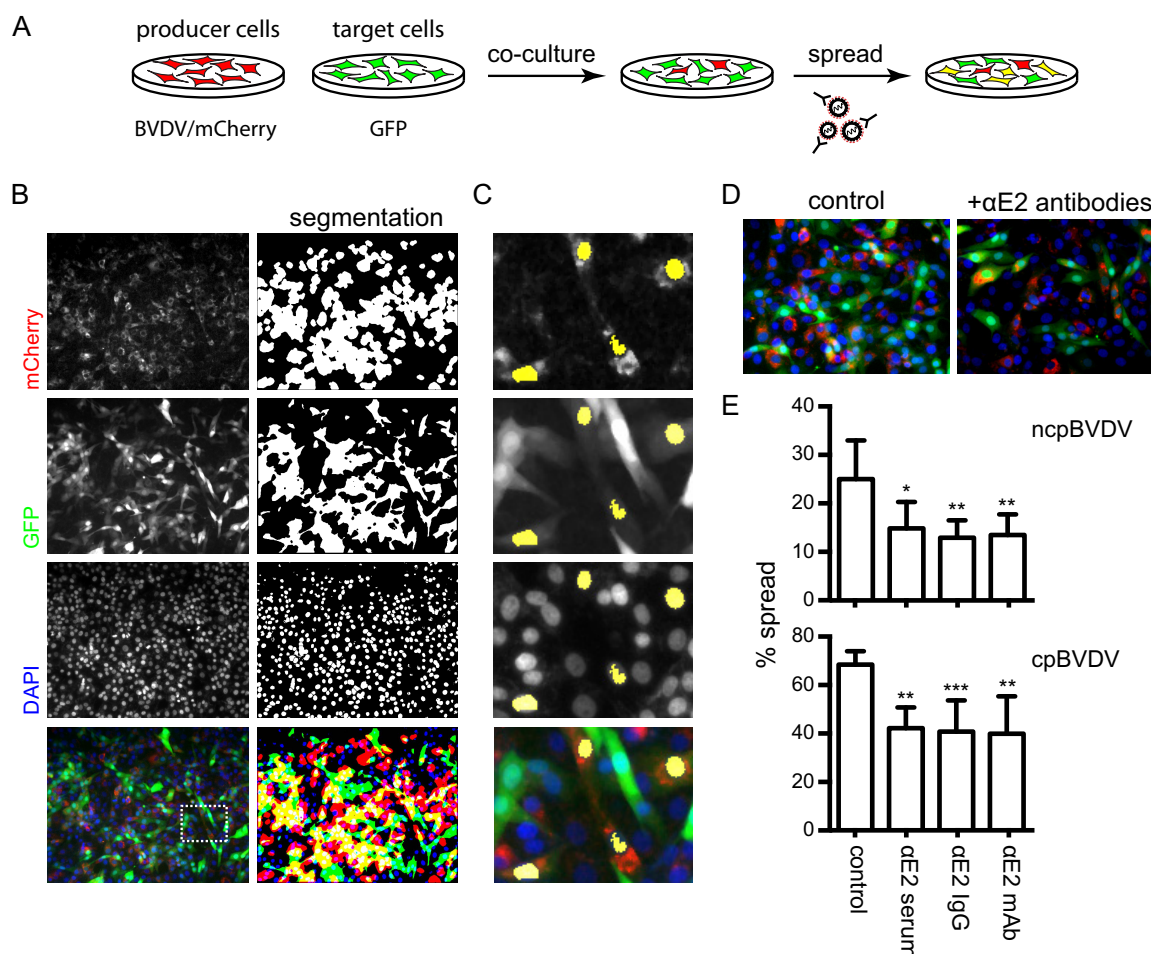


FIG 6 Cell-to-cell transmission of BVDV is the main mechanism contributing to spreading. (A) Schematic representation of the experimental setup of the coculture system of producer cells persistently infected with ncpBVDV/mCherry-E2 (red) and noninfected target cells expressing GFP (green). Spreading from producer cells to target cells can be distinguished by the expression of both GFP and mCherry (yellow). (B) Identification of infected target cells by automated image analysis. The number of target cells (GFP; green channel) infected with BVDV/mCherry-E2 (mCherry; red channel) was identified on a cell monolayer (DAPI; blue channel) by using the analytical tools of ImageJ software. Appropriate thresholding and binary processing of the red, green, and blue channels identified objects corresponding to mCherry expression in cpBVDV/mCherry-E2-infected cells, GFP expression in target cells, and cell nuclei, respectively (segmentation). We next used logical operators and “analyze particles” tools to number target cells (GFP and DAPI masks) and infected target cells (mCherry and GFP and DAPI masks). (C) Superposition of the result mask (yellow) identifying infected target cells with the split-channel images of the boxed area in panel B. (D) Direct cell-to-cell spread of BVDV. Representative images of spreading of BVDV into target cells in cocultures of producer (mCherry; red channel) and target (GFP; green channel) cells in control medium or medium containing neutralizing antibodies are shown. (E) Quantification of spreading. Bars represent the means and standard deviations of the percentages of target cells infected with ncp (top) or cp (bottom) BVDV/mCherry-E2 (% spread). At least a thousand total target cells were counted for each condition. Data were analyzed by one-way ANOVA with Dunnett's posttest (*, $P < 0.05$; **, $P < 0.01$; ***, $P < 0.001$).

antibody neutralization blocks spreading of free viruses, the comparison of spreading in the control and in the presence of antibodies allowed us to estimate the contribution of dissemination of free virus versus direct cell-to-cell transmission to BVDV spread. Our results indicate that direct cell-to-cell transmission accounts for nearly two-thirds of spreading. In a similar manner, when producer cells were infected with cpBVDV/mCherry-E2 and cocultured with noninfected target cells for 2 days, we observed that direct cell-to-cell transmission was the main mechanism contributing to BVDV spread (Fig. 6E).

Spread of BVDV from producer to target cells uses receptor-mediated clathrin-dependent endocytosis. We next asked whether cell-associated transmission of BVDV depends on the use of virus receptors. To address this question, we infected MDBK cells with BVDV/mCherry, and after washing of the noninternalized virus, cells were incubated with soluble E2 or with CD46 MAbs at concentrations that completely blocked

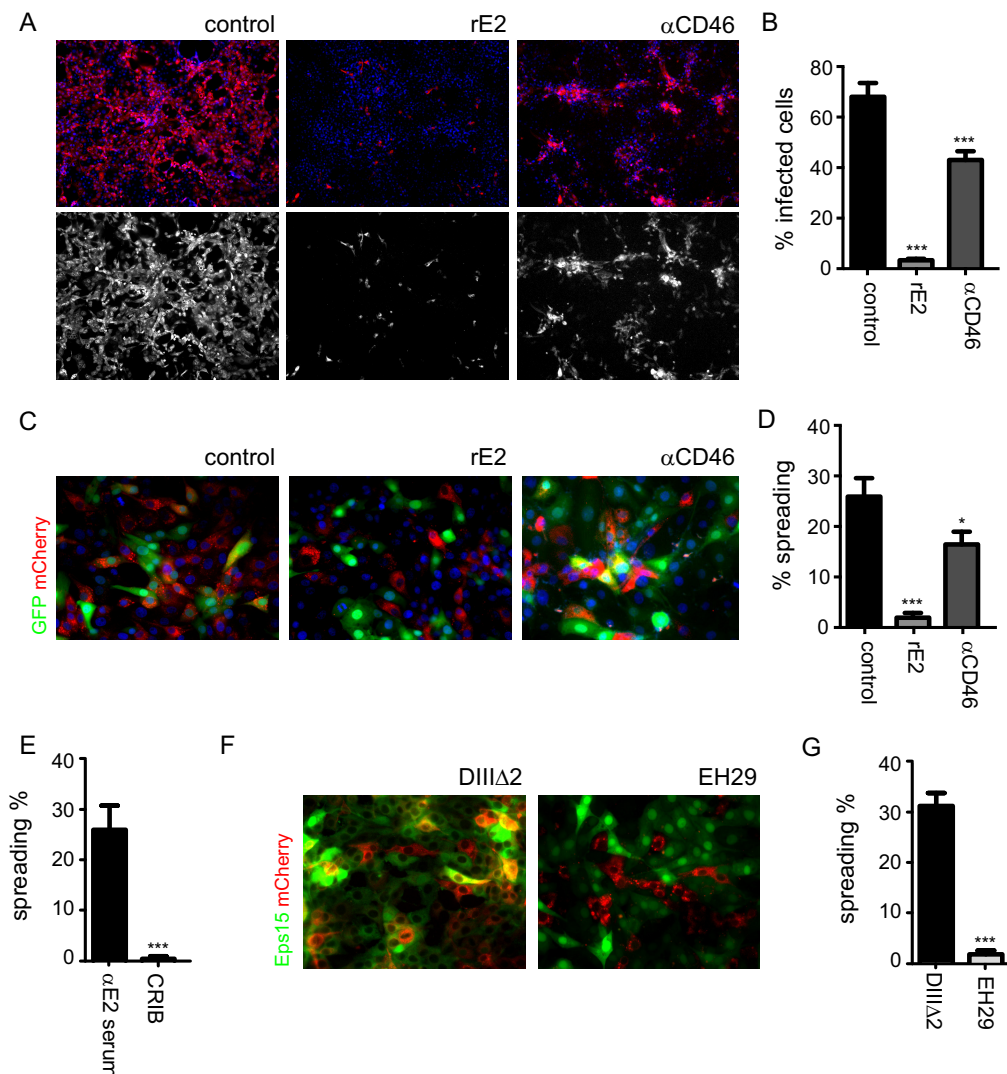


FIG 7 Cell-to-cell transmission of BVDV requires both receptor recognition and clathrin-dependent endocytosis. (A) Representative images of virus spread (red channel) in cells cultured in control medium or medium containing soluble E2 (rE2) or CD46 MABs (αCD46). (B) Bar graph showing quantification of the absolute percentage of infected cells. Bars represent the means and standard deviations for three independent images. Data were analyzed by one-way ANOVA with Dunnett's post-test (***, $P < 0.001$). (C) Representative images of producer (red channel; ncpBVDV/mCherry-E2) and target (green channel; GFP) MDBK cells in control cocultures (left) or cocultures in the presence of soluble E2 (middle) or CD46 MABs (right). (D) Quantification of spreading. Bars represent the means and standard deviations of the percentages of infected target cells. At least a thousand total target cells were counted for each condition. Data were analyzed by one-way ANOVA with Dunnett's post-test (*, $P < 0.05$; ***, $P < 0.001$). (E) Quantification of spreading from producer cells infected with ncpBVDV/mCherry-E2 (red channel) to target CRIB cells expressing GFP (green channel). Bars represent the means and standard deviations of the percentages of infected target cells. At least a thousand total target cells were counted for each condition. Data were analyzed by the unpaired t test (***, $P < 0.001$). (F) Representative images of producer MDBK cells cocultured with target MDBK cells overexpressing a control (DIIIΔ2) or dominant negative (EH29) Eps15 construct in the presence of neutralizing serum. (G) Quantification of spreading. Bars represent the means and standard deviations of the percentages of infected target cells. At least a thousand total target cells were counted for each condition. Data were analyzed by the unpaired t test (***, $P < 0.001$).

the entry of free virus and the infection was allowed to proceed for 2 days. We observed that foci of infection were confined to single cells after treatment with E2, suggesting that receptor occupancy prevents spreading (Fig. 7B). In striking contrast, foci of infection spread after the specific block of CD46, yielding a percentage of infected cells that was reduced to an extent similar to that for the treatment with neutralizing antibodies with respect to the control (compare Fig. 7B and Fig. 4E), implying that the function of CD46 is limited to the entry of free viruses. The requirement of receptor recognition for direct cell-to-cell transmission was further analyzed using the coculture

system. To this end, we set up cocultures in control medium or medium supplemented with soluble E2 or CD46 MAbs. We confirmed that soluble E2 completely blocked spreading, while efficient cell-to-cell transmission was measured in the presence of CD46 MAbs (Fig. 7C and D). Altogether, these experiments suggest that cell-to-cell spread of BVDV depends on the use of coreceptors for free virus entry or a specialized set of receptors.

As an alternative approach, we used CRIB cells as target cells in the coculture assay. CRIB cells are bovine cells derived from MDBK cells that, despite expressing CD46 on the surface, are nonsusceptible to BVDV infection due to a specific block of virus entry (45–47). We verified that CRIB cells were resistant to infection with BVDV by using an immunofluorescence assay to detect infected cells. In addition, recovery of infectious viruses after transfection of CRIB cells with *in vitro*-transcribed BVDV RNA confirmed that the cell line was permissive for virus replication (data not shown). Coculture of producer cells with CRIB cells stably expressing GFP showed that BVDV was not able to spread to CRIB cells, probably because of the lack of coreceptors that function in cell-associated spread on the target cell surface (Fig. 7E). Altogether, these results indicate that direct cell-to-cell transmission of BVDV requires receptor recognition on the target cell.

To study whether direct cell-to-cell transmission involves endocytosis of spreading viruses by the target cell, we analyzed spreading by using cocultures of producer cells and target cells expressing a control or dominant negative construct of Eps15 in the presence of neutralizing serum. We found that spreading to cells expressing the control construct was efficient. In contrast, the virus was not able to spread to target cells expressing the dominant negative construct, suggesting the requirement for clathrin-mediated endocytosis for direct cell-to-cell transmission of BVDV (Fig. 7F and G).

DISCUSSION

Direct cell-to-cell transmission of virus infections has emerged in recent years as a common theme in virus spread. Different viruses use disparate mechanisms of cell-to-cell transmission that usually rely on the assembly and exit of progeny virus (reviewed in references 26 and 27). Since assembled progeny viruses spread infection through the extracellular space, understanding the mechanisms supporting direct cell-to-cell versus cell-free transmission often requires suppressing free diffusion of viruses. Thus, cell culture models of virus spread in the presence of neutralizing antibodies that completely block cell-free virus are often used to study direct cell-to-cell transmission. Based on the dominance of BVDV E2 as an antigen in infected cattle, we expressed a recombinant version of E2 and generated neutralizing antibodies that were shown to completely block BVDV infection. We showed that BVDV spread in cultured MDBK epithelial cells was resistant to antibody neutralization when virus infection was initiated from either a virus stock or RNA transfection, thus providing evidence for direct cell-to-cell transmission of BVDV. Furthermore, resistance to antibody neutralization has been related to the use of tight cell-cell contacts for transmission. Confluent MDBK cells have well-developed adherens junctions and tight junctions (48), and in support of spreading through epithelial cell-cell contacts, we observed that spread was completely blocked by neutralizing antibodies when infected and uninfected cells were physically separated in a transwell coculture system.

Our study was based on the use of a pair of recombinant cp and ncp biotypes of the NADL strain of BVDV that carry a fusion of mCherry to the major envelope protein on the virus surface (E2), referred to as BVDV/mCherry-E2. In agreement with previous work reporting the insertion of small tags (such as the FLAG epitope or the 11-amino-acid subunit derived from NanoLuc luciferase) at this site (42, 43), we showed that insertion of mCherry yielded fully infectious virus particles. Furthermore, BVDV/mCherry-E2 used the authentic entry pathway of BVDV, as shown by comparing the effects of pharmacological and molecular inhibitors of virus entry on parental and recombinant viruses, indicating that the virus would be able to accommodate the foreign protein without compromising the function of E2. Therefore, this site of

insertion could be used to label virus particles that may aid in the study of pestivirus biology as well as the design of marker vaccine strains that allow differentiation of infected from vaccinated animals. Here we used only mCherry expression as a reporter for BVDV infection. Further characterization of our recombinant virus is still required to assess the potential for use in studies at the single-particle level.

To gain insight into the mechanisms that support spread of BVDV in cell culture, we used a fluorescence microscopy-based assay to unequivocally quantify spread from an infected to an uninfected cell. Our approach combined the coculture of producer cells infected with reporter BVDV/mCherry-E2 and target cells expressing GFP or GFP fusion proteins with automated image analysis. First, to estimate the contribution of cell-to-cell transmission to BVDV spread, we compared spreading in a control assay and that in the presence of neutralizing antibodies and found that antibody-resistant spread is the main mechanism contributing to propagation of BVDV infection in cell culture. This was the case for both the cp and ncp biotypes of BVDV, and differences in the absolute percentages of spreading between cp and ncp viruses can be attributed to the differences in replication kinetics of the two biotypes. Second, using complementary approaches, we showed the use of virus receptors for direct cell-to-cell spread. Even so, we observed that the BVDV receptor CD46 was dispensable for cell-associated spread of the virus. Interestingly, it was recently reported that receptors mediating attachment of free virus are dispensable for HCV cell-to-cell transmission, while postattachment receptors are required for both cell-free and cell-to-cell transmission (35–38). CD46 is the only identified BVDV receptor, and overexpression of CD46 in heterologous cell lines increases the attachment of BVDV, although it is not sufficient to turn cells susceptible to infection (8, 20). Moreover, evidence indicates that CD46 is not endocytosed (49). Therefore, it is possible that it functions as an attachment receptor for free viruses and that it is not required for cell-to-cell transmission, which depends on the use of postattachment receptors or coreceptors. Since E2 is the viral protein responsible for virus-receptor interaction, blocking of cell-to-cell transmission by use of soluble E2 suggests that E2 is required for cell-associated spread. In addition, the defect for direct transmission into CRIB cells indicates that virus receptors need to be recognized on the surfaces of target cells. Finally, using target cells expressing control and dominant negative constructs of Eps15, we determined that, as in the case of free viruses, infection of target cells depends on clathrin-mediated endocytosis. Overall, we demonstrated that BVDV uses direct cell-to-cell transmission as the main mode to propagate infection, and we showed that similar to entry of free viruses, this mode of propagation exploits cellular endocytic pathways dependent on clathrin.

Antibodies against BVDV prevent disease development following challenge. However, after exposure to the homologous virus, viremia and shedding of BVDV in nasal secretions still occur in the presence of serum neutralizing antibodies, suggesting that BVDV has developed strategies to overcome the host antibody response (17, 18). Thus, the demonstration of BVDV spread in the presence of neutralizing antibodies in cell culture sheds new light on the mechanisms employed by BVDV to evade antibody responses in immunocompetent adult animals. Direct cell-to-cell transmission can also explain the ability of ncp virus to cross the placental barrier and reach the fetus. In acute infection with BVDV, the virus is commonly isolated from peripheral blood mononuclear cells (PBMCs). Similar to transmission of HIV across the trophoblast layer of the placenta (50, 51), we speculate that the process of fetal infection may involve initial cell-to-cell transmission between infected PBMCs and trophoblasts.

Altogether, we propose a mechanism for BVDV cell-to-cell transmission that involves the egress of assembled virus particles in exocytic vesicles and their accumulation in the extracellular space at sites of cell-cell contact (52). Envelope glycoprotein E2 on the surfaces of extracellular viruses attached to the plasma membrane engages a cellular coreceptor on the target cell that mediates internalization of spreading virions by clathrin-dependent endocytosis.

milliliter as described by O'Reilly et al. (55). In order to verify that recombinant E2 was efficiently secreted, a fraction of the clarified supernatant was boiled in the presence of 1× cracking buffer (2% SDS, 10% glycerol, 60 mM Tris-HCl, pH 6.8, 0.1 M dithiothreitol [DTT]), and proteins were resolved by SDS-PAGE. Recombinant proteins were detected by Western blotting, employing both anti-6×His epitope tag (Rockland) and anti-BVDV antibodies. For final protein production, five T175 flasks were seeded with 2×10^7 Sf9 cells each and infected at a multiplicity of infection (MOI) of 5. E2 purification was performed with a Ni-Sepharose high-performance column (GE Healthcare) according to the manufacturer's instructions. Briefly, clarified supernatants were pooled and dialyzed into IMAC buffer (50 mM Tris, pH 7.6, 500 mM NaCl, 20 mM imidazole). After loading, protein fractions were eluted in a step gradient of imidazole and analyzed by SDS-PAGE and Coomassie blue staining.

Fluorescence microscopy. MDBK cells were seeded on glass coverslips at a density of 10^5 cells/well in 24-well plates and infected at an MOI of 0.1. At the indicated times after infection, cells were thoroughly washed and fixed using 4% paraformaldehyde (PFA). To analyze the correlation between mCherry and NS3 expression after infection with the cpBVDV/mCherry-E2 reporter, fixed samples were first incubated with a mouse antibody against NS3 and then washed three times in phosphate-buffered saline (PBS) before addition of an Alexa Fluor-conjugated secondary antibody. Cell nuclei were stained with DAPI (4',6-diamidino-2-phenylindole), and coverslips were then mounted onto glass slides by use of FluoroGuard antifade reagent (Bio-Rad). Samples were visualized under a Nikon Eclipse 80i fluorescence microscope equipped with a DS-Qi1Mc camera and analyzed with ImageJ software.

Confocal microscopy. Colocalization between mCherry and E2 in cells infected with cpBVDV/mCherry-E2 was assessed by confocal microscopy. Infected cells were fixed, stained with a monoclonal antibody against E2 (DMAB28412; Creative Diagnostics), and mounted onto glass slides. Images were acquired in a microscope with an inverted Olympus IX 81 module and a confocal FV1000 module with a Plan ApoN60X/1.42 objective controlled by the FV10-ASW 3.1 software program and were analyzed with ImageJ software.

BVDV entry assays. Monoclonal antibodies (MAbs) BVD/CA 17 and 26 against CD46 (56) were a kind gift from Till Rumenapf, University of Veterinary Medicine Austria. The effective concentrations for the inhibition of BVDV infection with recombinant E2 and CD46 MAbs were estimated in a cytopathic effect reduction assay (57). The inhibitory effect on virus entry was tested on MDBK cell monolayers incubated with recombinant E2 (1 µg/ml) and CD46 MAbs (3 µg/ml) for 1 h before infection with BVDV. Cells were thoroughly washed at 2 h, and the infection was allowed to proceed for 24 h. Fixed cells were stained and analyzed by fluorescence microscopy.

Drugs used in entry assays were first tested for cytotoxicity in MDBK cells. Cells in 96-well plates were incubated for 3 h with increasing amounts of drugs and rinsed twice with PBS, and after 72 h at 37°C, viability was measured using crystal violet staining as previously described (57).

To test the effects of drugs on BVDV entry, MDBK cells were preincubated for 1 h with increasing amounts of NH_4Cl (10 to 50 mM) or chlorpromazine (5 to 25 µM) (Sigma) in 200 µl of IM. Cells were then infected with BVDV for 2 h with the same amount of drug in the medium and rinsed 3 times with PBS, and after 24 h, the cells were fixed and visualized by fluorescence microscopy.

Lentivirus transduction and cell sorting. Due to the impossibility of transfecting MDBK cells with DNA, we used lentivirus transduction to express foreign proteins.

First, lentivirus transfer vectors coding for Eps15 DIIIΔ2 and Eps15 EH29 fused to GFP were constructed by subcloning the fragment between NheI and blunt-ended XbaI sites of the corresponding Eps15 constructs (58) into NheI and blunt-ended EcoRI sites of pLB (Addgene plasmid 11619).

To produce lentivirus, the transfer vector pLB coding for GFP, GFP-Eps15 DIIIΔ2, or GFP-Eps15 EH29 was cotransfected with the packaging vector pSPAX2 (Addgene plasmid 12260) and the vesicular stomatitis virus glycoprotein vector pMD2.G (Addgene plasmid 12259) into 293T cells by use of Lipofectamine 2000 according to the manufacturer's instructions. Supernatant with lentivirus was collected from one 10-cm dish 3 days after transfection, and low-speed concentration was performed by overnight centrifugation of the viral supernatant at $3,000 \times g$ and 4°C. Concentrated viral supernatants were supplemented with 20 mM HEPES, pH 7.4, and 10 µg/ml Polybrene (Sigma).

For MDBK transduction, 3×10^5 cells were seeded into 6-well plates. The following day, cells were washed with PBS and infected with lentiviruses by centrifugation at 2,500 rpm at 30°C for 30 min. After 4 h of incubation at 37°C, the medium was removed and complete fresh medium was added. GFP expression at 48 h was evaluated by fluorescence microscopy. Due to the low transduction efficiency of MDBK cells (5% to 10%), a round of enrichment of the cells expressing GFP was performed by cell sorting in a FACSAria II flow cytometer (BD Biosciences) to obtain a cell line with over 80% GFP-expressing cells.

In order to verify loss of function of clathrin-mediated endocytosis by expression of dominant negative Eps15, internalization of Texas Red-conjugated human transferrin (Rockland) into MDBK cells expressing GFP-Eps15 DIIIΔ2 or GFP-Eps15 EH29 was measured by fluorescence microscopy. Cells were serum starved for 30 min, incubated for 45 min with 15 µg/ml transferrin in serum-free medium at 37°C, rinsed three times with PBS, fixed with 4% PFA, and imaged.

BVDV neutralizing serum production and IgG purification. The purified recombinant E2 protein was used to generate a specific polyclonal antiserum. Four female mice of the CF1 strain were immunized following a standard immunization protocol. Briefly, mice were injected via the intraperitoneal route on days 0, 17, and 32, and sera were obtained at day 45. The first dose consisted of 2.5 µg of purified recombinant E2 mixed with an equal volume of Freund's complete adjuvant. The second and third doses consisted of 1.25 µg of protein mixed with an equal volume of Freund's incomplete adjuvant. All mice were bred in accordance with institutional animal guidelines under specific pathogen-free conditions in the local animal facility of the Instituto de Investigaciones

Biocientíficas at the Universidad Nacional de San Martín. Mouse experimentation was approved by the local regulatory agencies (CICUA-UNSAM).

Antibodies of the IgG isotype were purified from the serum by affinity chromatography. The serum was filtered through a 0.22- μ m-pore-size cellulose acetate membrane and loaded into a HiTrap protein G HP column (GE Healthcare) equilibrated with binding buffer (20 mM sodium phosphate, 150 mM sodium chloride). After washing with 10 column volumes of binding buffer, bound IgG antibodies were eluted in 10 column volumes of 0.1 M glycine, pH 2.5, and collected in 1-ml fractions in tubes containing 85 μ l 1 M Tris base. The eluted fractions were assayed for IgG heavy and light chains by SDS-PAGE and Coomassie blue staining. The fractions containing IgG antibodies were pooled, dialyzed into PBS, and concentrated by Centricon filtration.

Titration of neutralizing antibodies. Neutralizing titers were estimated by cytopathic effect reduction assays with the neutralizing serum, the purified IgG fraction, and an anti-BVDV MAb (DMAB28412; Creative Diagnostics) raised against E2. Briefly, wild-type cpBVDV was preincubated with serial dilutions of serum or antibodies for 30 min in infection medium. Virus was then added to a confluent MDBK cell monolayer in a 96-well microplate. After 72 h of incubation, cells were fixed and stained with a crystal violet solution (0.1% crystal violet, 20% ethanol) to measure the extent of cytopathic effect. The neutralizing antibody titer was estimated as the serum dilution capable of inhibiting the BVDV cytopathic effect by 90% (NT_{90}) compared to the control level.

Transwell coculture assay. MDBK cells were seeded on coverslips in a 24-well plate in the presence of 300 μ l of infection medium or medium supplemented with neutralizing serum (1:500). In a separate plate, 3×10^4 MDBK cells were seeded on transwell polycarbonate membrane inserts with a 3- μ m pore size (Corning), infected with ncpBVDV/mCherry-E2, and in turn cocultured with noninfected cells. After 48 h of incubation at 37°C, cells were fixed and processed for visualization by fluorescence microscopy.

Spreading assays in coculture systems. A coculture system to measure direct cell-to-cell transmission of the viral infection from infected cells to target noninfected cells was developed. To this end, we generated an MDBK cell line stably infected with ncpBVDV/mCherry-E2. MDBK cells were infected with the noncytopathic reporter virus, and after several passages, mCherry expression and the presence of infectious BVDV particles in the supernatant were successfully verified. Cocultures were set up by mixing infected producer cells (MDBK-mCherry) and labeled target cells expressing GFP or GFP fusion proteins (MDBK-GFP) at a 1:4 ratio. Cells were seeded on coverslips at a density of 10^5 cells/well in 500 μ l infection medium supplemented with neutralizing antibodies and incubated for 72 h before processing of the samples for fluorescence microscopy analysis. To measure spreading cpBVDV/mCherry-E2, MDBK cells were seeded on coverslips at a density of 30,000 cells/well and infected at an MOI of 3. At 2 h postinfection, cells were extensively washed, and MDBK-GFP cells were plated onto infected cells at a density of 10^5 cells/well in 500 μ l IM supplemented with neutralizing antibodies. Cocultures were fixed at 48 h and imaged as described below.

Computer-assisted image analysis. The number of virus-infected cells was determined by using the analytical tools of ImageJ software. The appropriate threshold for the red channel identified objects corresponding to mCherry expression in cpBVDV/mCherry-E2-infected cells. We next used the dilate tool and the particle analyzer to filter objects according to size and shape and to create a mask displaying only infected cells. Finally, we counted the number of cells obtained according to the filter.

Statistical analysis. Results represent independent repeats of the experiments, and statistical analyses were performed with GraphPad Prism 5 software. Inhibition plots were adjusted by nonlinear fitting, and columns in bar graphs were compared by the unpaired *t* test or by one-way analysis of variance (ANOVA) with the Dunnett's posttest.

ACKNOWLEDGMENTS

We thank Hervé Agaisse for a critical reading and discussion of the manuscript. Maria José Pascual assisted in the production of immune sera against E2.

This work was supported by a National Agency for the Promotion of Science and Technology (ANPCyT) grant (PICT2014-2213) to D.E.A.

REFERENCES

- Richter V, Lebl K, Baumgartner W, Obritzhauser W, Kasbohrer A, Pinior B. 2017. A systematic worldwide review of the direct monetary losses in cattle due to bovine viral diarrhoea virus infection. *Vet J* 220:80–87. <https://doi.org/10.1016/j.tvjl.2017.01.005>.
- Simmonds P, Becher P, Bukh J, Gould EA, Meyers G, Monath T, Muerhoff S, Pletnev A, Rico-Hesse R, Smith DB, Stapleton JT, ICTV Report Consortium. 2017. ICTV virus taxonomy profile: Flaviviridae. *J Gen Virol* 98:2–3. <https://doi.org/10.1099/jgv.0.000672>.
- Collett MS, Larson R, Belzer SK, Retzel E. 1988. Proteins encoded by bovine viral diarrhoea virus: the genomic organization of a pestivirus. *Virology* 165:200–208. [https://doi.org/10.1016/0042-6822\(88\)90673-3](https://doi.org/10.1016/0042-6822(88)90673-3).
- Tautz N, Tews BA, Meyers G. 2015. The molecular biology of pestiviruses. *Adv Virus Res* 93:47–160. <https://doi.org/10.1016/bs.aivir.2015.03.002>.
- Callens N, Brügger B, Bonnafous P, Drobecq H, Gerl MJ, Krey T, Roman-Sosa G, Rümenapf T, Lambert O, Dubuisson J, Rouillé Y. 2016. Morphology and molecular composition of purified bovine viral diarrhoea virus envelope. *PLoS Pathog* 12:e1005476. <https://doi.org/10.1371/journal.ppat.1005476>.
- Thiel HJ, Stark R, Weiland E, Rümenapf T, Meyers G. 1991. Hog cholera virus: molecular composition of virions from a pestivirus. *J Virol* 65:4705–4712.
- Liang D, Sainz IF, Ansari IH, Gil LH, Vassilev V, Donis RO. 2003. The envelope glycoprotein E2 is a determinant of cell culture tropism in ruminant pestiviruses. *J Gen Virol* 84:1269–1274. <https://doi.org/10.1099/vir.0.18557-0>.
- Maurer K, Krey T, Moennig V, Thiel HJ, Rümenapf T. 2004. CD46 is a cellular receptor for bovine viral diarrhoea virus. *J Virol* 78:1792–1799. <https://doi.org/10.1128/JVI.78.4.1792-1799.2004>.

9. Pande A, Carr BV, Wong SY, Dalton K, Jones IM, McCauley JW, Charleston B. 2005. The glycosylation pattern of baculovirus expressed envelope protein E2 affects its ability to prevent infection with bovine viral diarrhoea virus. *Virus Res* 114:54–62. <https://doi.org/10.1016/j.virusres.2005.05.011>.
10. Ridpath JF. 2013. Immunology of BVDV vaccines. *Biologicals* 41:14–19. <https://doi.org/10.1016/j.biologicals.2012.07.003>.
11. Thomas C, Young NJ, Heaney J, Collins ME, Brownlie J. 2009. Evaluation of efficacy of mammalian and baculovirus expressed E2 subunit vaccine candidates to bovine viral diarrhoea virus. *Vaccine* 27:2387–2393. <https://doi.org/10.1016/j.vaccine.2009.02.010>.
12. Ridpath JF. 2003. BVDV genotypes and biotypes: practical implications for diagnosis and control. *Biologicals* 31:127–131. [https://doi.org/10.1016/S1045-1056\(03\)00028-9](https://doi.org/10.1016/S1045-1056(03)00028-9).
13. Grooms DL. 2004. Reproductive consequences of infection with bovine viral diarrhoea virus. *Vet Clin North Am Food Anim Pract* 20:5–19. <https://doi.org/10.1016/j.cvfa.2003.11.006>.
14. Lanyon SR, Hill FI, Reichel MP, Brownlie J. 2014. Bovine viral diarrhoea: pathogenesis and diagnosis. *Vet J* 199:201–209. <https://doi.org/10.1016/j.tvjl.2013.07.024>.
15. Becher P, Tautz N. 2011. RNA recombination in pestiviruses: cellular RNA sequences in viral genomes highlight the role of host factors for viral persistence and lethal disease. *RNA Biol* 8:216–224. <https://doi.org/10.4161/rna.8.2.14514>.
16. Peterhans E, Bachofen C, Stalder H, Schweizer M. 2010. Cytopathic bovine viral diarrhoea viruses (BVDV): emerging pestiviruses doomed to extinction. *Vet Res* 41:44. <https://doi.org/10.1051/vetres/2010016>.
17. Lambot M, Joris E, Douart A, Lyaku J, Letesson JJ, Pastoret PP. 1998. Evidence for biotype-specific effects of bovine viral diarrhoea virus on biological responses in acutely infected calves. *J Gen Virol* 79:27–30. <https://doi.org/10.1099/0022-1317-79-1-27>.
18. Nobiron I, Thompson I, Brownlie J, Collins ME. 2003. DNA vaccination against bovine viral diarrhoea virus induces humoral and cellular responses in cattle with evidence for protection against viral challenge. *Vaccine* 21:2082–2092. [https://doi.org/10.1016/S0264-410X\(02\)00745-4](https://doi.org/10.1016/S0264-410X(02)00745-4).
19. Grummer B, Grotha S, Greiser-Wilke I. 2004. Bovine viral diarrhoea virus is internalized by clathrin-dependent receptor-mediated endocytosis. *J Vet Med Ser B* 51:427–432. <https://doi.org/10.1111/j.1439-0450.2004.00798.x>.
20. Krey T, Himmelreich A, Heimann M, Menge C, Thiel HJ, Maurer K, Rumenapf T. 2006. Function of bovine CD46 as a cellular receptor for bovine viral diarrhoea virus is determined by complement control protein 1. *J Virol* 80:3912–3922. <https://doi.org/10.1128/JVI.80.8.3912-3922.2006>.
21. Lecot S, Belouzard S, Dubuisson J, Rouille Y. 2005. Bovine viral diarrhoea virus entry is dependent on clathrin-mediated endocytosis. *J Virol* 79:10826–10829. <https://doi.org/10.1128/JVI.79.16.10826-10829.2005>.
22. El Omari K, Iourin O, Harlos K, Grimes JM, Stuart DI. 2013. Structure of a pestivirus envelope glycoprotein E2 clarifies its role in cell entry. *Cell Rep* 3:30–35. <https://doi.org/10.1016/j.celrep.2012.12.001>.
23. Krey T, Thiel HJ, Rumenapf T. 2005. Acid-resistant bovine pestivirus requires activation for pH-triggered fusion during entry. *J Virol* 79:4191–4200. <https://doi.org/10.1128/JVI.79.7.4191-4200.2005>.
24. Li Y, Modis Y. 2014. A novel membrane fusion protein family in Flaviviridae? *Trends Microbiol* 22:176–182. <https://doi.org/10.1016/j.tim.2014.01.008>.
25. Marsh M, Helenius A. 2006. Virus entry: open sesame. *Cell* 124:729–740. <https://doi.org/10.1016/j.cell.2006.02.007>.
26. Mothes W, Sherer NM, Jin J, Zhong P. 2010. Virus cell-to-cell transmission. *J Virol* 84:8360–8368. <https://doi.org/10.1128/JVI.00443-10>.
27. Sattentau Q. 2008. Avoiding the void: cell-to-cell spread of human viruses. *Nat Rev Microbiol* 6:815–826. <https://doi.org/10.1038/nrmicro1972>.
28. Johnson DC, Huber MT. 2002. Directed egress of animal viruses promotes cell-to-cell spread. *J Virol* 76:1–8. <https://doi.org/10.1128/JVI.76.1.1-8.2002>.
29. Yakimovich A, Gumpert H, Burckhardt CJ, Lutschg VA, Jurgeit A, Sbalzarini IF, Greber UF. 2012. Cell-free transmission of human adenovirus by passive mass transfer in cell culture simulated in a computer model. *J Virol* 86:10123–10137. <https://doi.org/10.1128/JVI.01102-12>.
30. Zhong P, Agosto LM, Munro JB, Mothes W. 2013. Cell-to-cell transmission of viruses. *Curr Opin Virol* 3:44–50. <https://doi.org/10.1016/j.coviro.2012.11.004>.
31. Taylor MP, Enquist LW. 2015. Axonal spread of neuroinvasive viral infections. *Trends Microbiol* 23:283–288. <https://doi.org/10.1016/j.tim.2015.01.002>.
32. Sewald X, Motamedi N, Mothes W. 2016. Viruses exploit the tissue physiology of the host to spread in vivo. *Curr Opin Cell Biol* 41:81–90. <https://doi.org/10.1016/j.ceb.2016.04.008>.
33. Sherer NM, Lehmann MJ, Jimenez-Soto LF, Horensavitz C, Pypaert M, Mothes W. 2007. Retroviruses can establish filopodial bridges for efficient cell-to-cell transmission. *Nat Cell Biol* 9:310–315. <https://doi.org/10.1038/ncb1544>.
34. Frischknecht F, Moreau V, Rottger S, Gonfloni S, Reckmann I, Superti-Furga G, Way M. 1999. Actin-based motility of vaccinia virus mimics receptor tyrosine kinase signalling. *Nature* 401:926–929. <https://doi.org/10.1038/44860>.
35. Brimacombe CL, Grove J, Meredith LW, Hu K, Syder AJ, Flores MV, Timpe JM, Krieger SE, Baumert TF, Tellinghuisen TL, Wong-Staal F, Balfe P, McKeating JA. 2011. Neutralizing antibody-resistant hepatitis C virus cell-to-cell transmission. *J Virol* 85:596–605. <https://doi.org/10.1128/JVI.01592-10>.
36. Carloni G, Crema A, Valli MB, Ponzetto A, Clementi M. 2012. HCV infection by cell-to-cell transmission: choice or necessity? *Curr Mol Med* 12:83–95. <https://doi.org/10.2174/156652412798376152>.
37. Timpe JM, Stamatakis Z, Jennings A, Hu K, Farquhar MJ, Harris HJ, Schwarz A, Desombere I, Roels GL, Balfe P, McKeating JA. 2007. Hepatitis C virus cell-cell transmission in hepatoma cells in the presence of neutralizing antibodies. *Hepatology* 47:17–24. <https://doi.org/10.1002/hep.21959>.
38. Witteveldt J, Evans MJ, Bitzegeio J, Koutsoudakis G, Owsianka AM, Angus AG, Keck ZY, Fount SK, Pietschmann T, Rice CM, Patel AH. 2009. CD81 is dispensable for hepatitis C virus cell-to-cell transmission in hepatoma cells. *J Gen Virol* 90:48–58. <https://doi.org/10.1099/vir.0.006700-0>.
39. Arenhart S, Flores EF, Weiblen R, Gil LH. 2014. Insertion and stable expression of Gaussia luciferase gene by the genome of bovine viral diarrhoea virus. *Res Vet Sci* 97:439–448. <https://doi.org/10.1016/j.rvsc.2014.07.007>.
40. Fan ZC, Bird RC. 2012. Development of a reporter bovine viral diarrhoea virus and initial evaluation of its application for high throughput antiviral drug screening. *J Virol Methods* 180:54–61. <https://doi.org/10.1016/j.jviromet.2011.12.011>.
41. Fan ZC, Dennis JC, Bird RC. 2008. Bovine viral diarrhoea virus is a suitable viral vector for stable expression of heterologous gene when inserted in between N(pro) and C genes. *Virus Res* 138:97–104. <https://doi.org/10.1016/j.virusres.2008.08.015>.
42. Tamura T, Fukuhara T, Uchida T, Ono C, Mori H, Sato A, Fauzyah Y, Okamoto T, Kurosu T, Setoh YX, Imamura M, Tautz N, Sakoda Y, Khromykh AA, Chayama K, Matsuura Y. 2018. Characterization of recombinant Flaviviridae viruses possessing a small reporter tag. *J Virol* 92:e01582-17. <https://doi.org/10.1128/JVI.01582-17>.
43. Wegelt A, Reimann I, Granzow H, Beer M. 2011. Characterization and purification of recombinant bovine viral diarrhoea virus particles with epitope-tagged envelope proteins. *J Gen Virol* 92:1352–1357. <https://doi.org/10.1099/vir.0.029330-0>.
44. Mendez E, Ruggli N, Collett MS, Rice CM. 1998. Infectious bovine viral diarrhoea virus (strain NADL) RNA from stable cDNA clones: a cellular insert determines NS3 production and viral cytopathogenicity. *J Virol* 72:4737–4745.
45. Flores EF, Donis RO. 1995. Isolation of a mutant MDBK cell line resistant to bovine viral diarrhoea virus infection due to a block in viral entry. *Virology* 208:565–575. <https://doi.org/10.1006/viro.1995.1187>.
46. Flores EF, Kreutz LC, Donis RO. 1996. Swine and ruminant pestiviruses require the same cellular factor to enter bovine cells. *J Gen Virol* 77:1295–1303. <https://doi.org/10.1099/0022-1317-77-6-1295>.
47. Krey T, Moussay E, Thiel HJ, Rumenapf T. 2006. Role of the low-density lipoprotein receptor in entry of bovine viral diarrhoea virus. *J Virol* 80:10862–10867. <https://doi.org/10.1128/JVI.01589-06>.
48. Palovuori R, Eskelinen S. 2000. Role of vinculin in the maintenance of cell-cell contacts in kidney epithelial MDBK cells. *Eur J Cell Physiol* 79:961–974. <https://doi.org/10.1078/0171-9335-00120>.
49. Maisner A, Zimmer G, Liszewski MK, Lublin DM, Atkinson JP, Herrler G. 1997. Membrane cofactor protein (CD46) is a basolateral protein that is not endocytosed. *J Biol Chem* 272:20793–20799. <https://doi.org/10.1074/jbc.272.33.20793>.
50. Arias RA, Muñoz LD, Muñoz-Fernández MA. 2003. Transmission of HIV-1 infection between trophoblast placental cells and T-cells take place via

- an LFA-1-mediated cell to cell contact. *Virology* 307:266–277. [https://doi.org/10.1016/S0042-6822\(02\)00040-5](https://doi.org/10.1016/S0042-6822(02)00040-5).
51. Lagaye S, Derrien M, Menu E, Coito C, Tresoldi E, Maucel P, Scarlatti G, Chaouat G, Barre-Sinoussi F, Bomsel M, European Network for the Study of In Utero Transmission of HIV. 2001. Cell-to-cell contact results in a selective translocation of maternal human immunodeficiency virus type 1 quasispecies across a trophoblastic barrier by both transcytosis and infection. *J Virol* 75:4780–4791. <https://doi.org/10.1128/JVI.75.10.4780-4791.2001>.
 52. Schmeiser S, Mast J, Thiel HJ, König M. 2014. Morphogenesis of pestiviruses: new insights from ultrastructural studies of strain Giraffe-1. *J Virol* 88:2717–2724. <https://doi.org/10.1128/JVI.03237-13>.
 53. Shaner NC, Campbell RE, Steinbach PA, Giepmans BN, Palmer AE, Tsien RY. 2004. Improved monomeric red, orange and yellow fluorescent proteins derived from *Discosoma* sp. red fluorescent protein. *Nat Biotechnol* 22:1567–1572. <https://doi.org/10.1038/nbt1037>.
 54. Unger T, Jacobovitch Y, Dantes A, Bernheim R, Peleg Y. 2010. Applications of the restriction free (RF) cloning procedure for molecular manipulations and protein expression. *J Struct Biol* 172:34–44. <https://doi.org/10.1016/j.jsb.2010.06.016>.
 55. O'Reilly DR, Miller LK, Luckow VA. 1994. Baculovirus expression vectors: a laboratory manual. Oxford University Press, New York, NY.
 56. Schelp C, Greiser-Wilke I, Wolf G, Beer M, Moennig V, Liess B. 1995. Identification of cell membrane proteins linked to susceptibility to bovine viral diarrhoea virus infection. *Arch Virol* 140:1997–2009. <https://doi.org/10.1007/BF01322688>.
 57. Pascual MJ, Merwaiss F, Leal E, Quintana ME, Capozzo AV, Cavasotto CN, Bollini M, Alvarez DE. 2018. Structure-based drug design for envelope protein E2 uncovers a new class of bovine viral diarrhoea inhibitors that block virus entry. *Antiviral Res* 149:179–190. <https://doi.org/10.1016/j.antiviral.2017.10.010>.
 58. Benmerah A, Bayrou M, Cerf-Bensussan N, Dautry-Varsat A. 1999. Inhibition of clathrin-coated pit assembly by an Eps15 mutant. *J Cell Sci* 112:1303–1311.